



Global Increase of the Intensity of Tropical Cyclones under Global Warming Based on their Maximum Potential Intensity and CMIP6 Models

Albenis Pérez-Alarcón^{1,2} · José C. Fernández-Alvarez^{1,2} · Patricia Coll-Hidalgo^{1,3}

Received: 3 March 2023 / Accepted: 23 May 2023 / Published online: 9 June 2023
© The Author(s) 2023

Abstract

Future changes in the intensity of tropical cyclones (TCs) under global warming are uncertain, although several studies have projected an upward trend in TC intensity. In this study, we examined the changes in the strength of TCs in the twenty-first century based on the Hurricane Maximum Potential Intensity (HuMPI) model forced with the sea surface temperature (SST) from the bias-corrected CMIP6 dataset. We first investigated the relationship between the mean lifetime maximum intensity (LMI) of major hurricanes (MHs) and the maximum potential intensity (MPI) using the SST from the Daily Optimum Interpolation SST database. The LMI of MHs and the MPI in the last two decades was, on average, 2–3% higher than mean values in the sub-period 1982–2000, suggesting a relationship between changes in MPI and LMI. From our findings, the projected changes in TC intensity in the near-future period (2016–2040) will be almost similar for SSP2-4.5 and SSP5-8.5 climate scenarios. However, TCs will be 9.5% and 17% more intense by the end (2071–2100) of the twenty-first century under both climate scenarios, respectively, compared with the mean intensity over the historical period (1985–2014). In addition, the MPI response to a warmed sea surface temperature per degree of warming is a 5–7% increase in maximum potential wind speed. These results should be interpreted as a projection of changes in TC intensity under global warming since the HuMPI formulation does not include environmental factors (i.e., vertical wind shear, mid-level moisture content and environmental stratification) that influence TC long-term intensity variations.

Highlights

- The maximum potential intensity (MPI) of tropical cyclones is a predictor of their climatological intensities.
- Tropical cyclones will be 17% more intense than today by the end of the 21st Century.
- The maximum potential wind speed will increase by 5–7%/°C under global warming.

Keywords Tropical cyclones · Climate change · Maximum potential intensity · Global warming · Climate scenarios · Sea surface temperature rise

1 Introduction

Tropical cyclones (TCs) are among the most devastating natural phenomena, causing lives and economic losses, due to strong winds, heavy rainfall, flash flooding and storm surge (Poulos 2010; Peduzzi et al. 2012; Gallina et al. 2016; Klotzbach et al. 2018). Overall, the impact of TCs has globally caused around 1.9 million death over the last two centuries, especially in coastal areas (Shultz et al. 2005; Mendelsohn et al. 2012; Hoque et al. 2017a, b, c).

Despite the long-term TC databases such as the Atlantic Hurricane Database (HURDAT2; Landsea and Franklin 2013) included in the International Best Track Archive for Climate Stewardship (IBTrACS; Knapp et al. 2010, 2018), the inhomogeneities in TC records (Chang and Guo 2007; Vecchi and Knutson 2008; Kossin et al. 2013; Bhatia et al. 2019) prevent the detection of reliable climatic signals in the variability of TC activity both at the basins and on a global scale (Emanuel 2021a). Therefore, the influence of climate change on TC activity remains uncertain (Peduzzi et al. 2012; Moon et al. 2019; Knutson et al. 2019, 2020).

While some studies in the last decades have found an increase in the percentage of Category 4–5 hurricanes on the Saffir–Simpson wind scale (e.g., Webster et al. 2005; Elsner et al. 2008; Holland and Bruyère 2014), other works have considered this trend part of the interdecadal variations in the frequency of intense TCs related to fluctuations in the atmospheric environment (Chan 2006; Li et al. 2015; Yan et al. 2017) or detected a non-significant upward trend (Klotzbach and Landsea 2015). Most recently, Kossin et al. (2020) noted a significant upward trend in the exceedance probability and proportion of major hurricanes (MHs, Category 3+ on the Saffir–Simpson scale) but Pérez-Alarcón et al. (2021a) and Vecchi et al. (2021) found a no robust long-term trend in TCs reaching hurricane category over the North Atlantic (NATL) basin. On the contrary, Klotzbach et al. (2022) detected a downward trend in the global number of hurricanes from 1990 to 2021. For further details, readers can consult a recent book by Chu and Murakami (2022), which updates and describes changes in TC activity.

Numerous studies (e.g., Emanuel et al. 2008; Camargo 2013; Murakami et al. 2014; Satoh et al. 2015; Wehner et al. 2015; Knutson et al. 2020; Roberts et al. 2020; Emanuel 2021b; Chand et al. 2022) have also revealed changes in TC frequency in future climate. For example, Camargo (2013), using 14 models from phase 5 of the Coupled Model Intercomparison Project (CMIP5), found that all of the models underestimated the global frequency of TCs and presented a wide range of global TC frequency. Murakami et al. (2014) found a marked decrease in TC frequency in the basins of the Southern Hemisphere, Bay of Bengal, Western North Pacific (WNP), Central and East Pacific (NEPAC), and the Caribbean Sea and increases in the Arabian Sea and the subtropical central Pacific Ocean. Likewise, Roberts et al. (2020), using the sixth-generation Coupled Climate Model Intercomparison Project (CMIP6) HighResMIP Multimodel Ensemble, found that TC activity generally will decrease in the South Indian Ocean by 2050, while changes in the other basins are more sensitive to tracking algorithms. On this basis, most of the previous findings highlighted a robust reduction in global TC frequency as a response to global warming. In contrast, few studies using dynamical models (Bhatia et al. 2018; Vecchi et al. 2019) or statistical–dynamical downscaling (Emanuel and Sobel 2013; Lee et al. 2020) recently detected that the frequency of TCs shifts to higher values as the twenty-first century progresses.

Additionally, several studies (e.g., Mendelsohn et al. 2012; Emanuel and Sobel 2013; Yin et al. 2013; Fraza and Elsner 2015; Walsh et al. 2016, 2019; Bhatia et al. 2018;

Knutson et al. 2020; Lee et al. 2020; Emanuel 2021b; Pérez-Alarcón et al. 2021b) have also projected an increase in the intensity of TCs under different climate change scenarios. In this line, Bhatia et al. (2018) found that the TC intensification rate is projected to be higher by the end of this century relative to the present day, leading to more MHs. Emanuel (2021b) found an increase in the severity of TCs using CMIP6, and Knutson et al. (2020) stated that climate change is probably increasing the intensity of TCs. Nevertheless, future changes in TC activity depend on the uncertainties in climate projections, such as climate-forcing scenarios, model dynamics, physics and spatial resolutions (Roberts et al. 2018).

The linkages between climate and TC intensity could be examined through the maximum potential intensity (MPI) of TCs (Emanuel 1986), which is generally taken as the upper TC intensity limit (Walsh et al. 2019). Previous studies have analytically derived equations for the MPI with processes that possibly affect TC intensity, such as convective available potential energy in the eyewall region (Bister and Emanuel 2002), effects of dry air intrusion into the core (Tang and Emanuel 2010), effects of the ocean mixing under TC forcing (Miyamoto et al. 2017), the environmental stratification (Kieu and Zhang 2018), and the friction in the atmospheric boundary layer (Pérez-Alarcón et al. 2021c, 2022). All these previous MPI approaches were based on the classical Emanuel's MPI theory representing the TC as a Carnot heat engine. Recent works by Kieu and Wang (2017ab) considered the basic scales of hurricanes as dynamical variables to derive a low-order hurricane model, which leads to an estimate of the MPI different from the classic Carnot cycle approach. According to Kieu and Zhang (2018), this low-order model could lead to an MPI equilibrium and its asymptotical stability, which cannot be achieved by working with a steady-state assumption as in the previous studies (e.g., Emanuel 1986; Bister and Emanuel 2002).

Emanuel and Sobel (2013) highlighted that the TC potential intensity variations using the Carnot cycle approach are likely more dependent on the SST than other forcing conditions. It is important to remark that TCs generally cannot achieve their MPI due to several negative environmental factors, such as vertical wind shear (Frank and Ritchie 2001; Alland et al. 2021a, b; Sharma and Varma 2022; Wang and Tan 2022), entrainment of dry air (Shu and Wu 2009; Luo and Han 2021; Shi et al. 2019; Wang and Toumi 2019), and sea surface temperature (SST) cooling from air-sea interaction (Pun et al. 2013; Yang et al. 2020; Pasquero et al. 2021). Nonetheless, based on the MPI theory, several works have addressed the increasing intensity of future TCs. For example, Korty et al. (2008) found a significant increase and poleward expansion of MPI. Wing et al. (2015) detected robust trends of TC MPI in the NATL basin over the period 1980–2013, suggesting that the environment could support intense TCs circa to the upper limit. Knutson et al. (2020) addressed that the projected increase in TC intensity with SST warming by about 1–10% for a 2 °C is supported by the MPI trends. Park et al. (2021) examined the MPI over the area of TC passage to South Korea using CMIP5 and CMIP6 models. Pérez-Alarcón et al. (2021b) applied the Hurricane Maximum Potential Intensity model (HuMPI; Pérez-Alarcón et al. 2021c, 2022) forced with the SST from the Geophysical Fluid Dynamics Laboratory – Climatic Model version 4.0 (Held et al. 2019) to investigate the projected changes in the TC MPI over the NATL basin for 2050, 2075 and 2100 under the extreme Shared Socio-Economic Pathways (SSPs) 5–8.5 (SSP5-8.5; O'Neill et al. 2017; Riahi et al. 2017). Pérez-Alarcón and Fernández-Alvarez (2022) also investigated the climatological variations in the intensity of TCs formed over the NATL basin by applying the HuMPI model. These authors found an increase of 3.89% and 3.20% in the last 20 seasons (2002–2021) relative to the period 1982–2001 for MHs and MPI, respectively.

Even though theory and modeling studies suggest an increase in TC intensity on the basin-wide and global scales in a warming climate, there are uncertainties in the projected responses of TC intensity to climate change (Knutson et al. 2019, 2020). For further details, readers can also refer to the review paper by Wu et al. (2022), which provides a comprehensive state-of-art of the effect of climate change on TC intensity. Additionally, despite variety of negative influences not fully accounted for by the MPI theory, previous works (Emanuel 2000; Wing et al. 2007; Bryan and Rotunno 2009; Kossin and Camargo 2009; Wang et al. 2014; Gilford et al. 2017, 2019) have noted that the potential intensity theory could be used as a predictor for the climatological intensities of TCs. Therefore, this work seeks to examine the changes in TC intensity both at the basins and on a global scale based on the MPI under the CMIP6 SSP2-4.5 and SSP5-8.5 scenarios during the twenty-first century by applying the HuMPI model. The SSP2-4.5 and SSP5-8.5 scenarios represent, respectively, the intermediate challenges scenario with a radiative stabilization rate of 4.5 Wm^2 beyond 2100 and the high challenges scenario with emissions high enough to produce a radiative forcing of 8.5 Wm^2 in 2100. These “medium” and “high” scenarios have been used for many previous projections summarized by the Intergovernmental Panel on Climate Change (Widhalm et al. 2018). Additionally, detailed descriptions of the CMIP6 SSPs can be found in O’Neill et al. (2017) and Eyring et al. (2016) which provide an overview of the experimental design of CMIP6.

The rest of the paper includes in Section 2 the databases and methodology applied in this work and a description of the HuMPI model. The results and discussion are provided in Sections 3 and 4, respectively, and the conclusions and plans for future works are provided in Section 5.

2 Materials and Methods

2.1 Data

To feed the HuMPI model, we used the SST from the Bias-corrected CMIP6 global dataset for the SSP2-4.5 and SSP5-8.5 scenarios from 1979 to 2100 (Xu et al. 2021) with a horizontal grid spacing of $1.25^\circ \times 1.25^\circ$. This database was constructed based on 18 models from the most up-to-date Global Circulation Models CMIP6 (see Xu et al. 2021) and the European Centre for Medium-Range Weather Forecasts Reanalysis 5 (ERA5) reanalysis (Hersbach et al. 2020). In summary, the bias-corrected method applied to this dataset decomposed Global Circulation Models and reanalysis data into long-term trends and anomalies. The long-term trend was estimated using the multi-model ensemble (Dai et al. 2020) mean derived from 18 CMIP6 models over historical (1979–2014) and future (2015–2100) periods. The 18 CMIP6 models used to construct the Bias-corrected CMIP6 dataset are listed in Table 1 according to their equilibrium climate sensitivity (ECS) from lowest to highest. The ECS is defined as the global mean temperature change following double CO_2 concentrations (Nijssen et al. 2020; Zelinka et al. 2020).

In addition, we utilized the Daily Optimum Interpolation SST (OISST) database v2.1 (Banzon et al. 2020) with $0.25^\circ \times 0.25^\circ$ horizontal resolution to evaluate the changes in the MPI in the four past decades. We also used the TCs records from 1982 to 2020 from the United States warning agency best tracks: the National Hurricane Center/Central Pacific Hurricane Center (HURDAT2; Landsea and Franklin 2013) for NATL and Central and East Pacific (NEPAC) basins and the Joint Typhoon Warning Center (JTWC; Chu et al. 2002) for the remaining

Table 1 CMIP6 models used by Xu et al. (2021) to construct the Bias-corrected CMIP6 global dataset. ECS: equilibrium climate sensitivity (in °C). The ECS was obtained from Nijse et al. (2020)

Model	ECS	Institution	Region
MIROC6	2.56	Japan Agency for Marine-Earth Science and Technology	Japan
GFDL-ESM4	2.68	Geophysical Fluid Dynamics Laboratory,	USA
NorESM2-LM	2.69	Norwegian Climate Center	Norway
MPI-ESM1-2-LR	2.77	Max Planck Institute for Meteorology	Germany
FGOALS-fg3	2.80	Institute of Atmospheric Physics, Chinese Academy of Sciences	China
MPI-ESM1-2-HR	2.99	Max Planck Institute for Meteorology	Germany
FGOALS-f3-L	3.00	Institute of Atmospheric Physics, Chinese Academy of Sciences	China
AWI-CM-1-1-MR	3.20	Alfred Wegener Institute, Helmholtz Centre for Polar and Marine Research	Germany
BCC-CSM2-MR	3.07	Beijing Climate Center	China
MRI-ESM2-0	3.14	Meteorological Research Institute, Japan Meteorological Agency	Japan
ACCESS-ESM1-5	3.97	Commonwealth Scientific and Industrial Research Organisation	Australia
EC-Earth	4.22	European EC-Earth Consortium	Europe
EC-Earth3-Veg	4.34	European EC-Earth Consortium	Europe
IPSL-CM6A-LR	4.63	Institute Pierre Simon Laplace	France
ACCESS-CM2	4.81	Commonwealth Scientific and Industrial Research Organisation	Australia
CESM2-WACCM	4.90	Climate and Global Dynamics Laboratory	USA
CEMS2	5.30	Climate and Global Dynamics Laboratory	USA
CanESM5	5.66	Canadian Centre for Climate Modelling and Analysis	Canada

global basins. It is worth noting that both agencies are from the United States, which guarantees homogeneity in the estimation of the TC intensity as the one-minute average wind speed at an altitude of 10 m.

2.2 Description of HuMPI model

The HuMPI model was developed by Pérez-Alarcón et al. (2021c), and it is based on the classic potential intensity theory of TCs (E-PI theory) proposed by Emanuel (1986). The E-PI theory assumes that the steady mature TC has an axisymmetric structure with flows that satisfy both hydrostatic and gradient wind balances, and is in a state of slantwise moist neutral condition (Emanuel 1986; Wu et al. 2022). Overall, HuMPI is divided into two parts: the first represents the thermodynamic part and the second the dynamic part. The thermodynamic part assumes that the TC acts as a generalized Carnot heat engine requiring the SST as input. The potential maximum wind speed (V_{max}) at the top of the boundary layer (BL) can be expressed as:

$$V_{max}^2 = \frac{T_b - T_{00}}{T_b} \frac{C_k}{C_d} (h_s^* - h_b^*) \quad (1)$$

where T_b (in K) is the temperature at the top of the BL, T_{00} (in K) is the outflow temperature, C_k/C_d is the ratio between the surface exchange coefficient for enthalpy and the surface drag coefficient, $(h_s^* - h_b^*)$ is the difference between the saturation moist static energy (in m^2/s^2) at the sea surface and the saturation moist static energy above the BL. Following

Emanuel (2004), variations in h_b^* at constant altitude are related to variations in the saturation entropy. By the first law of thermodynamics, we obtain:

$$\alpha_1 V_{max}^2 + \alpha_2 V_{max} + \alpha_3 = 0 \tag{2}$$

where

$$\alpha_1 = 1 - \frac{1}{2} \frac{C_k}{C_d} \tag{3}$$

$$\alpha_2 = \frac{-1}{2} f r_m \tag{4}$$

$$\alpha_3 = \frac{-T_b - T_{00}}{T_b} \frac{C_k}{C_d} (h_s^* - h_a) - \frac{C_k}{C_d} T_{00} R_d \ln \frac{P_m}{P_a} + \frac{1}{4} \frac{C_k}{C_d} f^2 r_a^2 \tag{5}$$

where r_m (in m) is the radius of maximum wind speed, r_a (in m) is the outer limit of the vortex, P_m and P_a (in Pa) are the surface pressures at r_m and r_a , respectively, f (in s^{-1}) is the Coriolis parameter, and h_a is the BL moist static energy. Solving (Eq. 2) and considering only the positive solution, we can estimate V_{max} (in m/s) at the top of the BL.

The dynamic part of the HuMPI model is based on the TC BL model proposed by Smith (2003) and revised by Smith and Vogl (2008). Taking the integral of the BL equations for a steady axisymmetric vortex in a homogeneous fluid on an f-plane (see Eqs. 1–4 in Smith 2003) with respect to z from the surface to the top of the BL and assuming that the BL has uniform depth (δ , in m) and constant density, the equations for radial (u) and azimuthal (v) components of wind speed (in m/s) are obtained:

$$\frac{du}{dr} = \frac{w_{\delta-}}{\delta} + \frac{v_{gr}^2 - v^2}{ru} - f \left(\frac{v_{gr} - v}{u} \right) - \frac{C_d}{\delta} \sqrt{u^2 + v^2} \tag{6}$$

$$\frac{dv}{dr} = \frac{w_{\delta-}}{u\delta} (v_{gr} - v) - \left(\frac{v}{r} + f \right) - \frac{v C_d}{u\delta} \sqrt{u^2 + v^2} \tag{7}$$

where v_{gr} (in m/s) is the tangential wind speed, $w_{\delta-} = (w_{\delta} - |w_{\delta}|)/2$, w_{δ} is the vertical velocity (in m/s) at the top of the BL. The assumption of gradient wind balance for the tangential wind speed has been considered the major deficiency of the E-PI theory (Smith et al. 2008; Kowaleski and Evans 2016; Makarieva and Nefiodov 2023). Therefore, to compute tangential wind speed (v_{gr}), the HuMPI uses the radial wind profile developed by Willoughby et al. (2006). This radial wind profile depends on the V_{max} , which was taken from Eq. (2). By assuming that the wind speed in surface is quite similar to the wind speed in the BL, and solving Eqs. (6)-(7), we computed the maximum potential wind speed (MPWS) as the maximum of $\sqrt{u^2 + v^2}$. To estimate the minimum potential central pressure (MPCP), we used the pressure radial profile developed by Fernández-Alvarez et al. (2019). Note that MPWS (MPCP) theoretically establishes the upper (lower) limit for the maximum wind speed (minimum central pressure) that a TC can reach.

HuMPI was previously used by Pérez-Alarcón et al. (2021b) to investigate the impact of global warming on the MPI of TCs formed over the NATL basin. It is worth noting that HuMPI estimates the limit of TC intensity if the large-scale factors are favorable for TC intensification. Note that real TC intensity is affected by both dynamic and thermodynamic

factors. In some of the basins, dynamic factors are more important than thermodynamic factors to TC intensification, i.e., the WNP basin (Chan 2009).

2.3 Methodology

The annual average of SST, maximum potential wind speed (MPWS) and minimum potential central pressure (MPCP) were computed for each basin using the grid points inside the red boxes shown in Fig. 1. That is, from 5°N to 35°N and the eastern coast of America to 1°W for the NATL, from 5°N to 30°N and the western coast of America to 180°W for NEPAC, from 5°N to 30°N and 100°E to 180°E for WNP, from 5°N to 25°N and the northeastern coast of Africa coast to 100°E for North Indian Ocean (NIO), from 5°S to 30°S and the southeastern coast of Africa to 135°E for the South Indian Ocean (SIO); and from 5°S to 30°S and 135°E to 120°W for the South Pacific Ocean (SPO). Although several works (Shen et al. 2018; Sun et al. 2019; Zhang et al. 2018) have identified the long-term poleward shift of TC, the criterion of selection of these regions was based on the fact that TCs generally reached the hurricane category on the Saffir–Simpson wind scale in these areas, as indicated by purple points in Fig. 1.

To gain an overview of the relationship between the lifetime maximum intensity (LMI) of TCs that reached the MH category and the MPI, we first performed the HuMPI estimations fed by the SST from the OISST dataset from 1982 to 2020, and second, we divided this period into two sub-periods. The length of each sub-period was determined based on the SST anomalies in each basin. We applied the pruned exact linear time (PELT) method (Killick et al. 2012) to detect a change point in the SST anomalies, as shown in Fig. 2. Thus, based on the PELT algorithm, we divided the 1980–2020 time frame into 1982–2002 and 2003–2020 for NATL and NEPAC, 1982–2001 and 2002–2020 for NIO and SIO and 1982–2000 and 2001–2020 for WNP and SPO basins. Hereafter, the first sub-period is namely SP1 and the second SP2. We then computed the increase of the mean SST, MH intensity, and MPI in the period SP2 relative to period SP1. For this analysis, we only utilized from best track archives the LMI of MHs for which MPI is most relevant. We refer to LMI as the first time a TC reaches its maximum intensity during its lifetime, following Emanuel (2000) and Gilford et al. (2019).

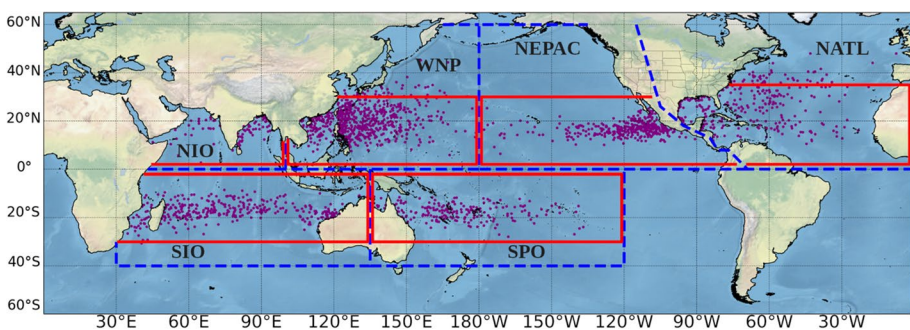


Fig. 1 Study region. The dashed blue lines denote the boundaries of each basin. The red lines represent the areas for computing the annual average sea surface temperature, maximum potential wind speed and minimum potential central pressure

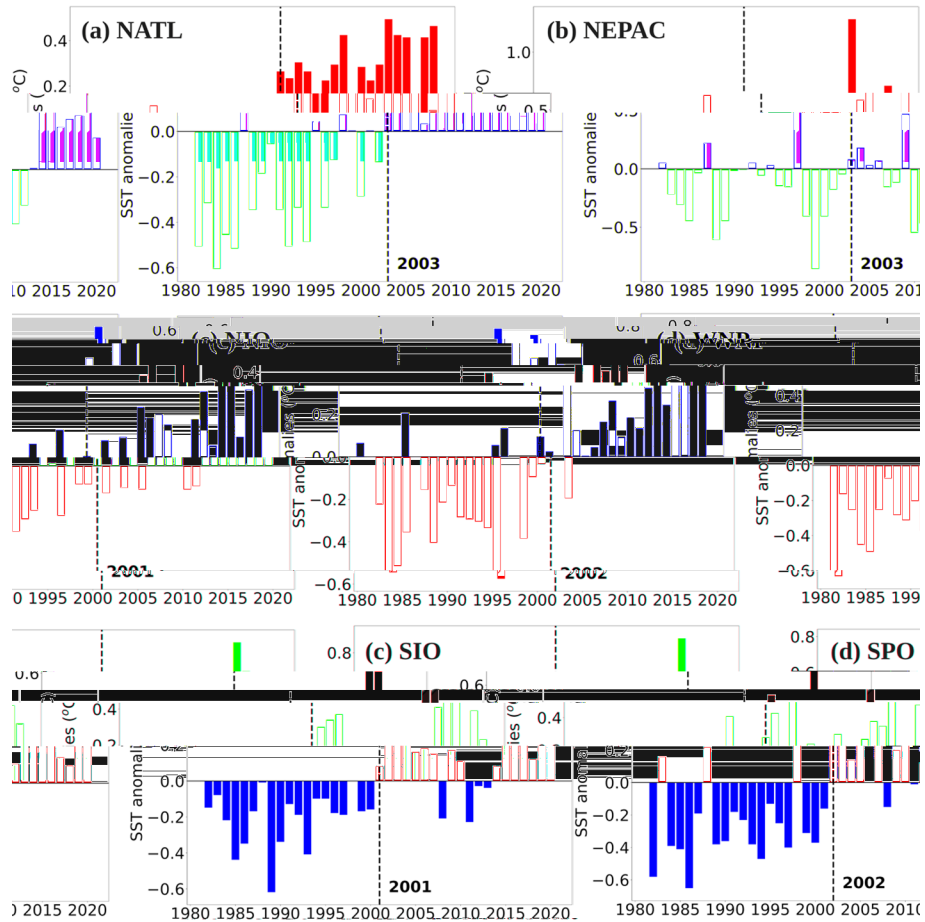


Fig. 2 Annual sea surface temperature (SST) anomalies ($^{\circ}\text{C}$) from 1982 to 2020 in (a) North Atlantic (NATL), (b) Central and East Pacific (NEPAC), (c) North Indian Ocean (NIO), (d) Western North Pacific (WNP), (e) South Indian Ocean (SIO), (f) South Pacific Ocean (SPO). The SST anomalies were computed as the differences between the annual SST and the mean SST from 1982 to 2020. The annual SST values were computed using the grid points within the red lines in Fig. 1. The vertical black dashed line illustrates the change point detected in the SST anomalies

Additionally, we conducted MPI estimations using the HuMPI model forced with the SST from the historical and future periods from the bias-corrected CMIP6 dataset for the SSP2-4.5 and SSP5-8.5 scenarios. We then estimated the changes in the MPI relative to the historical period. Following recommendations from the World Meteorological Organization (WMO), a 30-year period is the most appropriate length to perform climatological analysis (Lai and Dzombak 2019). Therefore, we examined the SST, MPWS and MPCP in three 30-year periods, namely historical (HIST, 1985–2014), mid (MID, 2041–2070) and end (END, 2071–2100) of the twenty-first century. Additionally, TC prediction for the near-future period (usually, a time scale of 10–30 years) has recently received attention from researchers in this field (e.g., Kim et al. 2012; Choi et al. 2016; Li et al. 2017). Thus, we also analyzed these variables in the 25-year near-future period (2016–2040).

TC activity is distinctly marked by a strong seasonal cycle. Therefore, the annual mean values were averaged in each basin during the most active period of the TC season, as shown by Dwyer et al. (2015) and Sobel et al. (2021), from August to October in NATL, from July to September in NEPAC, from July to October in WNP, from January to March in SIO and SPO. For the NIO basin, as the TC activity shows a bimodal monthly distribution, the annual average was computed using May, October, and November.

Additionally, to reduce the influence of the interannual variability on the response of SST, MPWS and MCPC to climate warming, we applied an 11-year time window moving average for each year from 2015 to 2100. Note that five years from the historical period were used for estimating the variables' values in 2015 (the mean from 2010 to 2020). Similarly, it occurred in 2016, 2017, 2018, and 2019 but using 4, 3, 2 and 1 years, respectively, from the historical period. Additionally, as the Bias-corrected CMIP6 global dataset used to force the HuMPI model is available until 2100, we reduced the time window for the moving average to 9, 7, 5, and 3 years as we approached 2100. For example, the value in 1999 is the average from 1998 to 2100, while in 2100 is the average of 1999 and 2100.

3 Results

3.1 Changes in the Intensity of TCs from 1982 to 2020

Figure 3 displays the increment within the most active period of the TC season of the mean SST from the OISST dataset, LMI and MPWS in the period SP2 relative to the period SP1. The rising of average SST ranged from 1.2% to 2.0% in the Northern Hemisphere, with the highest increment in NATL and NIO basins, while the changes in SST varied from 1.2% to 1.9% in the basins in the Southern Hemisphere (SIO and SPO). Note from Fig. 3 that the LMI exhibited the highest increment in the NEPAC basin with 6.2%, while the MPWS showed the largest changes in NATL (3.4%) and SIO (3.0%).

Table 2 shows trends in the SST, LMI and MPWS in a regional and global scales during the peak of TC season in each basin from 1982 to 2020. While the SST exhibited an increasing trend ($p < 0.05$) in all basins (Table 2), we only found a statistically significant increase in the LMI of MHs in NEPAC, WNP, SIO and SPO. In addition, the SST has globally increased by 0.20 °C/decade and the LMI by 1.1 m/s per decade. Furthermore, the MPWS has increased from 0.7 m/s to 1.2 m/s per decade, with the most notable increase

Fig. 3 Changes (in percentage) of the mean Sea Surface Temperature (SST), lifetime maximum intensity (LMI) of major hurricanes intensity (Category 3+ hurricanes on the Saffir–Simpson wind scale) and maximum potential wind speed (MPWS) in the period SP2 relative to the period SP1. See the Methodology section and Fig. 2 for references in the time frame of periods SP1 and SP2 in each basin

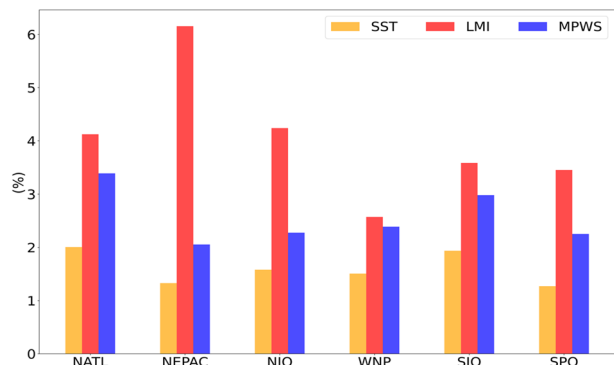


Table 2 Trends in the mean sea surface temperature (SST, in °C/decade), lifetime maximum intensity (LMI, in m/s per decade) of major hurricanes (category 3+ on the Saffir–Simpson wind scale) and maximum potential wind speed (MPWS, in m/s per decade) from 1982 to 2020 using the OISST, best-track datasets and HuMPI model, respectively. Note that these trends were computed during the peak of TC season in each basin. Values with an * are statistically significant at 95% confidence level

Variable	NATL	NEPAC	NIO	WNP	SIO	SPO	Global
SST	0.25*	0.16*	0.21*	0.23*	0.22*	0.17*	0.20*
LMI	1.1	1.8*	1.1	0.9*	0.9*	1.1*	1.1*
MPWS	1.2*	0.8*	0.9*	1.1*	0.9*	0.7*	0.9*

in NATL (1.2 m/s per decade), and WNP (1.1 m/s per decade) basins, while the globally increase was 0.9 m/s per decade. Note that we did not analyze the changes in the minimum central pressure due to several missing values in the JTWC best track archives.

Figure 3 reveals that an increase in the LMI of MHs in SP2 agrees with an increasing SST. Similarly, during SP2, the MPI has increased relative to SP1. Note that the changes in the LMI were computed using the observational records from the best track archives. Thus, changes in LMI are also controlled by dynamics factors (e.g., vertical wind shear), which are not included in the MPI estimations, as noted above. Previously Sobel et al. (2016) addressed that MPI provide a useful guide to the statistical distribution of actual intensities achieved by real TCs. Therefore, although the growth fractions are different, an increase in the MPI suggests an increase in the LMI of MHs. This behavior confirms previous findings addressed by Emanuel (2000) and Gilford et al. (2019), who stated that the MPI could be used as a predictor of the climatology intensity of TCs. Guo and Tan (2018) noted that the MPI is strongly tied to the change in TC intensity and locations. In addition, although most TCs do not reach their MPI, some observational evidences suggest that variations of LMI are consistent with variations in MPI (Emanuel 2000; Wing et al. 2007).

3.2 Trends in the MPI of TCs Using the HIST Period from the Bias-corrected CMIP6 Dataset

We also computed trends in SST and MPI variables using the annual mean values in each basin from the outputs from the HuMPI model forced with the SST from the HIST period. During 30-year HIST period (1985–2014), the bias-corrected SST exhibited an upward trend ($p < 0.05$) slightly lower than the tendency found using the OISST dataset. Overall, the SST increased from 0.11 °C/decade (in SPO) to 0.21 °C/decade (in NATL), while the globally upward trend was 0.17 °C/decade.

Likewise, the MPWS showed a statistically significant ($p < 0.05$) upward trend in response to the increase in SST, ranging from 0.50 m/s per decade (in SIO) to 1.3 m/s per decade (in WNP). Additionally, the globally increased of the MPWS was 0.83 m/s per decade, which is quite similar to that found using the OISST dataset. The MPCP exhibited a small significant downward trend, varying from 0.70 hPa/decade to 1.45 hPa/decade. Table 3 summarizes these findings. Similar MPI trends were previously found by Song and Klotzbach (2018) using TC records from 1961 to 2016 of the WNP basin, which is consistent with the continuous warming of the tropical WNP SST.

It is worth noting that these mean values were exclusively computed using the data during the peak of the TC season in each basin (see Methodology section), not for

Table 3 Trends in the mean sea surface temperature (SST, in °C/decade), maximum potential wind speed (MPWS, in m/s per decade) and minimum potential central pressure (MPCP, in hPa/decade) from 1985 to 2014 using the SST from the bias-corrected CMIP6 dataset during historical simulations. All values are statistically significant at 95% confidence level

Variable	NATL	NEPAC	NIO	WNP	SIO	SPO	Global
SST	0.21	0.19	0.16	0.20	0.17	0.11	0.17
MPWS	1.09	0.91	0.70	1.30	0.80	0.50	0.83
MPCP	-1.45	-1.18	-0.91	-1.40	-1.10	-0.70	-1.1

the whole TC season. Therefore, climatological MPI differs from the operational MPI (e.g., daily MPI reported by the Center for Ocean-Land-Atmosphere studies at <http://wxmaps.org/pix/hurpot.html> or by the Department of Meteorology of the Higher Institute of Technologies and Applied Sciences, University of Havana, for the NATL basin at <https://www.instec.cu/model/HuMPI.php>) or climatological MPI using the full TC season. We use these mean values as a baseline to project the changes in the MPI and, therefore, TC intensity under the SSP2-4.5 and SSP5-8.5 climate scenarios.

3.3 Projected Changes in the Intensity of TCs

The percent increment in the SST, MPWS and MPCP during the future period (2015–2100) relative to their mean values in the HIST period is shown in Fig. 4. The SST will increase by about 1.5–2.5% in the near-future, 4–5% in the mid-century and 6.5–8% by the end of the twenty-first century under the SSP2-4.5 climate scenario, as revealed in Fig. 4. In response, the MPWS will be 3.5–4.5%, 5.5–7.5% and 8.5–10.5% higher in the near-future, mid and end of the twenty-first century than its mean values in the HIST period, respectively, while the MPCP will decrease by about 0.5%, 0.6% and 1.2%, respectively. Overall, we detected that the SST will increase at a rate of 0.62–0.80%/decade, while the projected trend in MPWS and MPCP will be 1.1–1.3%/decade and -0.1–0.2%/decade, respectively.

Figure 4 also reveals for the near-future period, the projected changes in SST and MPI are almost similar in each basin under both climate scenarios. Under the extreme climate scenario SSP5-8.5, the increase in SST and MPWS will be approximately 1.5–1.7 times higher than their respective values under the SSP2-4.5 scenario at the END period. The SST will increase by 10–11% (5–6%) at the end (mid) of the twenty-first century. Meanwhile, the MPWS will be 9–11% (MID) and 15–18% (END) higher than its mean values in the HIST period. Likewise, the MPCP will decrease by 1.1–1.8% and 2.1–2.8%, respectively.

Emanuel and Sobel (2013) and Wing et al. (2015) stated that trends in MPI are primarily explained by trends in air-sea thermodynamic disequilibrium. Figure 4 also shows that the increasing rate of mean MPI is slightly larger than that of mean SST. Given that the MPI formulation in HuMPI model does not depend on mid-level moisture, the result indicates that temperature in the upper troposphere play an important role in controlling the MPI of TCs.

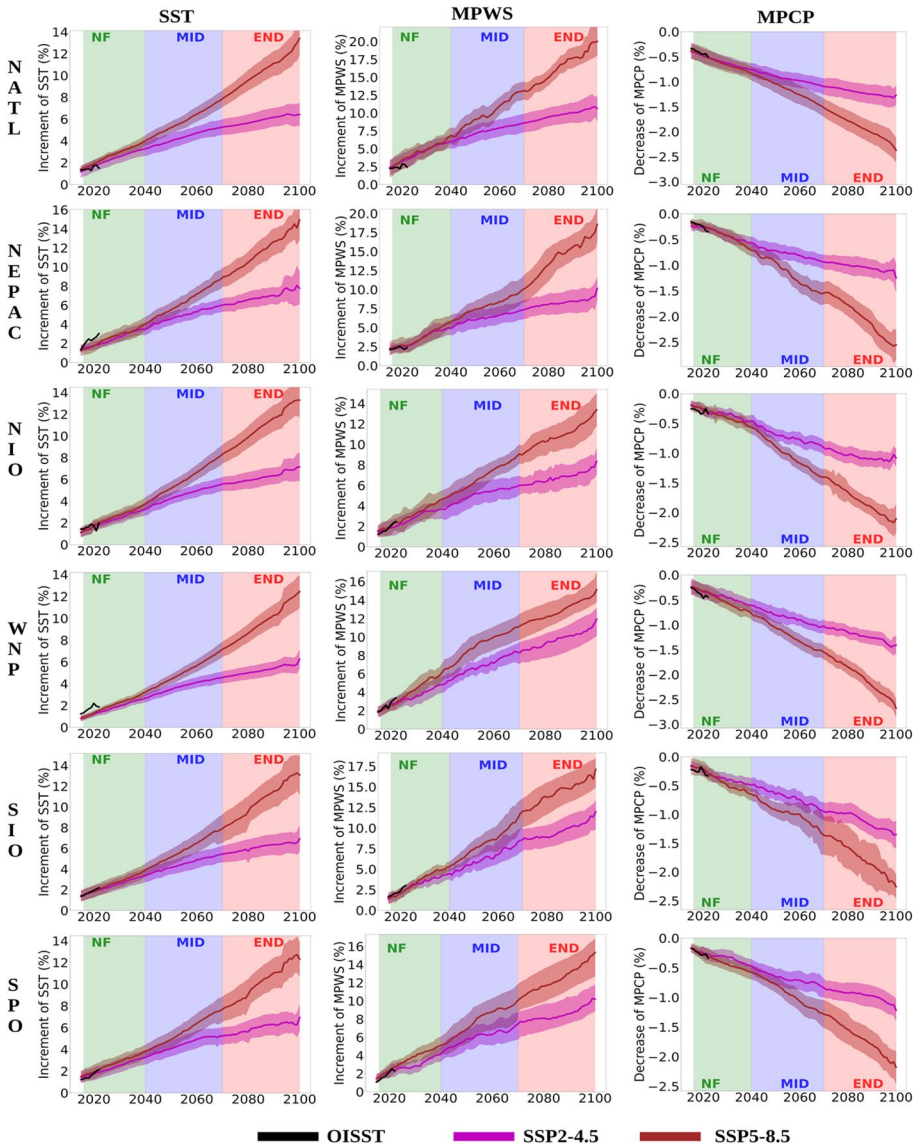


Fig. 4 Changes (in percentage) of the mean Sea Surface Temperature (SST), maximum potential wind speed (MPWS) and minimum potential central pressure (MPCP) in the period 2015–2100 under the SSP2-4.5 and SSP5-8.5 climate scenarios relative to the historical period (1985–2014). Green, blue and red shaded areas denote the time frame for the near-future (NF, 2016–2040), MID (2041–2070) and END (2071–2010) periods. The black, purple and brown solid lines denote the SST from the OISST dataset and SSP2-4.5 and SSP5-8.5 scenarios from the bias-corrected CMPI6 dataset, respectively. The purple and brown shaded areas represent the 95% confidence interval (CI) for the projected changes in SST, MPWS and MPCP under the SSP2-4.5 and SSP5-8.5 scenarios, respectively. The CI was computed using the SST from CMIP6 models listed in Table 1 and the corresponding HuMPI simulations

4 Discussion

By applying a linear regression between SST and MPWS, we detected that the MPWS increases by about 5–7%/°C under global warming, which is interestingly similar with the expected increase in low-level atmospheric water vapour based on the Clausius–Clapeyron relationship. Several authors (e.g., Braun et al. 2012; Ge et al. 2013; Tao and Zhang 2014) have addressed the role of atmospheric moisture in TCs genesis and intensification. Other studies (e.g., Held and Soden 2006; O’Gorman and Muller 2010; Knutson et al. 2020) have noted that under climate change and according to the Clausius–Clapeyron relationship, the low-level atmospheric water vapor will increase by about 6–7%/°C.

Figure 5 shows that the spatial pattern of the projected increase in SST and MPWS and the projected decrease in MPCP agrees with the future annual changes of these variables shown in Fig. 4. This confirms the projected increase of SST previously discussed in tropical regions over which TCs generally occur. Consequently, it is observed that all basins exhibit extreme values of MPWS and MPCP by the END period under the SSP5-8.5 scenario. In addition, the projected changes over the NATL basin confirms previous findings by Pérez-Alarcón et al. (2021b).

Interestingly, the largest projected changes in SST, MPWS and MPCP are observed north and south of 20° of latitude in both hemispheres (Fig. 5). This behavior supports the future poleward expansion of TC activity (Zhao and Held 2012; Murakami et al. 2012) due to changes in

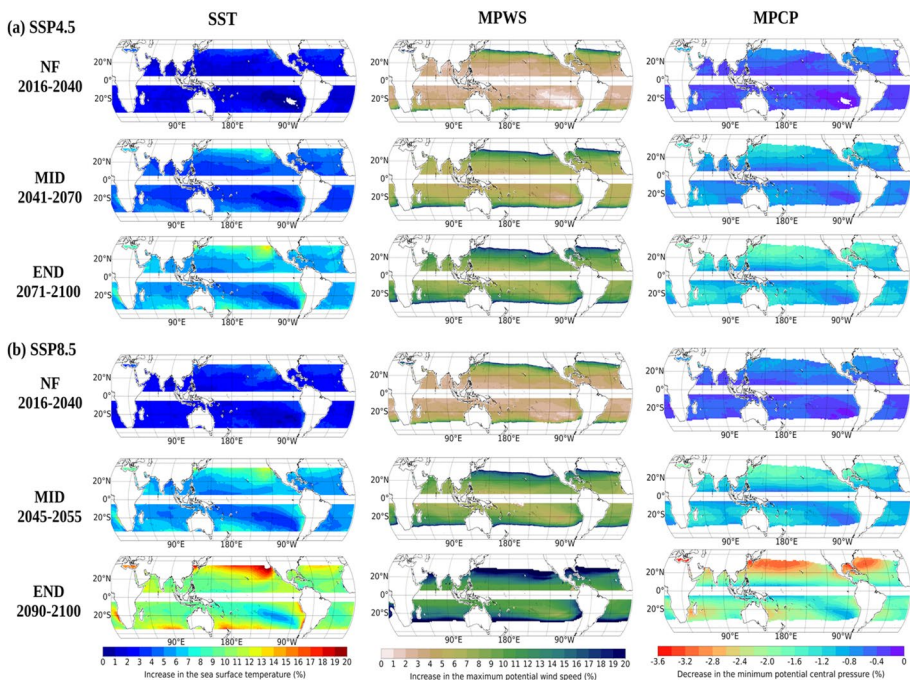


Fig. 5 Projected increase (%) in the sea surface temperature (SST) and maximum potential wind speed (MPWS) and projected decrease (%) in the minimum potential central pressure (MPCP) for the near-future (NF, 2016–2040), MID (2041–2070) and END (2071–2100) of twenty-first century under the (a) SSP2-4.5 and (b) SSP5-8.5 climate scenarios. These projections were computed using as baseline the historical period (1985–2014) and are statistically significant at 95% confidence level

the meridional structure of favorable environmental conditions for TCs development (Wu et al. 2014; Grise et al. 2018; Sharmila and Walsh 2018). According to Sharmila and Walsh (2018), regional variations of the Hadley circulation favor the expansion of the tropics providing beneficial conditions for poleward development of TCs. Overall, there is increasing evidence that the spatial distribution of future SST changes and associated tropical circulation changes play a modulator role in the projected responses of TC intensity (Knutson et al. 2013; Murakami et al. 2012; Wu et al. 2014; Sharmila and Walsh 2018; Studholme et al. 2022).

Our findings agree with previous works that investigated future changes in TC intensity. For example, Bloemendaal et al. (2022) detected an increase in TC intensity ranging from 7.2% to 23.8% by combining the benefits of high-resolution global climate models (GCMs) with synthetic TC modeling. Meanwhile, Thompson et al. (2021) applied the pseudo-global warming method to investigate Bejisa-like cyclones in future environments over the SPO basin. They found that the intensity will be 6.5% more intense on average by the end of the twenty-first century than in the present climate. Note that we projected an increase in TC intensity over the SPO basin by 6–7% and 8–12% under SSP2-4.5 and SSP5-8.5 climate scenarios (Fig. 4), respectively. Using a similar approach, Delfino et al. (2023) found that the intensity of TCs-like Typhoons Haiyan, Bopha, and Mangkhut over the WNP basin will increase by 14%, 4%, and 12%, respectively, under the SSP5-8.5 scenario. Our results support this previous finding by projecting an increase of TC intensity over the WNP basin by approximately 9.8% and 12.9% at the MID and END of the twenty-first century under the high emissions scenario (SSP5-8.5). Although slightly high, our results also confirm and support the findings of Knutson et al. (2019), who projected an increase in TC intensity by about 1–10% derived from synthesizing the results from many GCM-based studies.

Due to the dominant role of SST in determining the MPI based on the Emanuel MPI theory, these results provide insights into the projected changes in the intensity of TCs. Nevertheless, observational and modelling studies showed that large-scale factors play an essential role in TC long-term intensities variations (e.g., Kieu and Zhang 2018). Dynamics factors can inhibit a TC from reaching its MPI, as previously noted by Kossin (2017) and Kossin et al. (2020). For example, vertical wind shear can affect the thermal structure of a TC and limit its intensification (e.g., Wu and Emanuel 1993; Jones 1995; Frank and Ritchie 2001; Fraza and Elsner 2015). Although this work did not investigate changes in dynamic factors that influence TC activity under global warming, a recent study by Lockwood et al. (2022) using CMIP6 models found a negative correlation between MPI and vertical wind shear. Further studies are required to understand the response of large-scale parameters to global warming that modulate TC activity. Additionally, a limitation in several Global Circulation Model projections of future TC activity is the lack of realistic air-sea interaction processes due to simulations with specified SSTs rather than coupled ocean–atmosphere simulations (Walsh et al. 2019). It is important to highlight that CMIP6 models have achieved encouraging progress over the previous phases of the Coupled Model Intercomparison Project (Li et al. 2020; Zhou et al. 2020; Fu et al. 2021). Recently, Yang and Huang (2022) noted that CMIP6 models notably improved air-sea interactions.

5 Conclusions

This work analyzed the changes in the intensity of TCs under the Shared Socio-Economic Pathways (SSPs) 2–4.5 and 5–8.5 climate scenarios based on the Hurricane Maximum Potential Intensity (HuMPI) model estimations. For investigating the relationship between

the lifetime maximum intensity (LMI) of major hurricanes (MHs) and the maximum potential intensity (MPI), we fed HuMPI with the sea surface temperature (SST) from the Daily Optimum Interpolation SST database. To compute the annual mean values of LMI, SST and MPI in various basins, we extracted these variables in the months of the maximum frequency of TC activity in each region, i.e., from August to October in the North Atlantic (NATL) basin, from July to September in the Central and East Pacific (NEPAC), from July to October in the Western North Pacific (WNP), from January to March in the South Indian Ocean (SIO) and the South Pacific Ocean (SPO), and in May and from October to November in the North Indian Ocean (NIO). We also applied the pruned exact linear time (PELT) algorithm to detect a change point in SST anomalies time series in each basin to subdivide the 1982–2020 period into two sub-periods (SP1 and SP2). We found that changes in the average MPI in the SP2, relative to the SP1, were reflected in the changes in the LMI of MHs, which confirmed that the MPI is an important predictor of the climatological intensities of TCs, in agreement with previous research findings.

We forced the HuMPI model with the SST from the Bias-corrected CMIP6 global dataset to detect future changes in the intensity of TCs. From our findings, TCs will be 6.5% (10%) and 9.5% (17%) more intense by the MID (2041–2070) and the END (2071–2100) of the twenty-first century under SSP2-4.5 and SSP5-8.5 scenarios compared with the average MPI over the HIST period (1985–2014), respectively. The largest changes in SST and MPI were detected north and south of 20° of latitude in both hemispheres, which supports the projected poleward shift of TC activity due to the expansion of the tropics. Overall, we detected that the maximum potential wind speed increases by about 5–7%/°C under global warming. These findings should be interpreted as a projection of changes in TC intensity in a warmer climate. The HuMPI formulation did not include environmental factors that play essential roles in TC long-term intensity variations, such as vertical wind shear, mid-level moisture content and environmental stratification. Additionally, our results are affected by the uncertainties in climate projections, i.e., climate-forcing scenario and model dynamics, physics and resolutions.

In future work, we will include in the study the projected changes in large-scale parameters that affect the intensity of TCs, such as vertical wind shear and moisture content in the atmosphere as well as in the climatic variability modes, to have more details on how global warming will influence the activity of the TCs in each basin and on a global scale.

Acknowledgements The authors acknowledge the availability of public datasets from the National Hurricane Center and the NOAA/NCDC, JTWC and Science Data Bank. We also thank Oscar Díaz-Rodríguez from the Instituto de Ciencias de la Atmósfera y Cambio Climático, UNAM, for his comments to improve the manuscript. This work has been also possible thanks to the computing resources and technical support provided by CESGA (Centro de Supercomputación de Galicia). We also acknowledge the funding for open access from the Universidade de Vigo/Consortio Interuniversitario do Sistema Universitario de Galicia.

Author Contributions All authors contributed to the study conception and design. Material preparation data analysis were performed by A. Pérez-Alarcón, J. C. Fernández-Alvarez and P. Coll-Hidalgo. The first draft of the manuscript was written by Albenis Pérez-Alarcón and all authors commented on previous versions of the manuscript. All authors read and approved the final manuscript.

Funding Open Access funding provided thanks to the CRUE-CSIC agreement with Springer Nature.

Data Availability The datasets used in this study are freely available. The HURDAT2 database is accessible from <https://www.nhc.noaa.gov/data/#hurdat>. The JTWC best track archive was retrieved from <https://www.metoc.navy.mil/jtwc/jtwc.html?best-tracks>, the Bias-corrected CMIP6 global dataset is public available at <https://doi.org/10.11922/sciencedb.00487>, the Daily Optimum Interpolation Sea Surface Temperature database is available at <https://www.ncdc.noaa.gov/oisst>. The Python code from HuMPI model can be obtained from <https://doi.org/10.5281/zenodo.6475215> or directly from the Github repository at <https://github.com/apalarcon/HuMPI-master>.

Declarations

Competing Interests The authors declare that they have no known competing financial interests or personal relationships that could have appeared to influence the work reported in this paper.

Ethics Approval Not applicable.

Consent to Participate Not applicable.

Consent to Publish Not applicable.

Open Access This article is licensed under a Creative Commons Attribution 4.0 International License, which permits use, sharing, adaptation, distribution and reproduction in any medium or format, as long as you give appropriate credit to the original author(s) and the source, provide a link to the Creative Commons licence, and indicate if changes were made. The images or other third party material in this article are included in the article's Creative Commons licence, unless indicated otherwise in a credit line to the material. If material is not included in the article's Creative Commons licence and your intended use is not permitted by statutory regulation or exceeds the permitted use, you will need to obtain permission directly from the copyright holder. To view a copy of this licence, visit <http://creativecommons.org/licenses/by/4.0/>.

References

- Alland JJ., Tang BH, Corbosiero KL, Bryan GH (2021a) Combined effects of midlevel dry air and vertical wind shear on tropical cyclone development. Part I: Downdraft ventilation. *J Atmos Sci* 78(3):763–782 <https://doi.org/10.1175/JAS-D-20-0054.1>
- Alland JJ, Tang BH, Corbosiero KL, Bryan GH, (2021b) Combined effects of midlevel dry air and vertical wind shear on tropical cyclone development. Part II: Radial ventilation. *J Atmos Sci* 78(3):783–796 <https://doi.org/10.1175/JAS-D-20-0055.1>
- Banzon V, Smith TM, Steele M, Huang B, Zhang HM (2020) Improved estimation of proxy sea surface temperature in the Arctic. *J Atmos Ocean Technol* 37(2):341–349. <https://doi.org/10.1175/JTECH-D-19-0177.1>
- Bhatia KT, Vecchi GA, Knutson TR, Murakami H, Kossin J, Dixon KW, Whitlock CE (2019) Recent increases in tropical cyclone intensification rates. *Nat Commun* 10(1):1–9. <https://doi.org/10.1038/s41467-019-08471-z>
- Bhatia K, Vecchi G, Murakami H, Underwood S, Kossin J (2018) Projected response of tropical cyclone intensity and intensification in a global climate model. *J Clim* 31(20):8281–8303. <https://doi.org/10.1175/JCLI-D-17-0898.1>
- Bister M, and Emanuel KA (2002) Low frequency variability of tropical cyclone potential intensity 1. Inter-annual to interdecadal variability. *J Geophys Res Atmos* 107(D24):4801 <https://doi.org/10.1029/2001JD000776>
- Bloemendaal N, de Moel H, Martinez AB, Muis S, Haigh ID, van der Wiel K, et al. (2022) A globally consistent local-scale assessment of future tropical cyclone risk. *Sci Adv* 8(17):eabm8438 <https://doi.org/10.1126/sciadv.abm8438>
- Braun SA, Sippel JA, Nolan DS (2012) The impact of dry mid-level air on hurricane intensity in idealized simulations with no mean flow. *J Atmos Sci* 69:236–257. <https://doi.org/10.1175/JAS-D-10-05007.1>
- Bryan GH, Rotunno R (2009) The maximum intensity of tropical cyclones in axisymmetric numerical model simulations. *Mon Wea Rev* 137:1770–1789. <https://doi.org/10.1175/2008MWR2709.1>
- Camargo SJ (2013) Global and regional aspects of tropical cyclone activity in the CMIP5 models. *J Clim* 26(24):9880–9902. <https://doi.org/10.1175/JCLI-D-12-00549.1>
- Chan JC (2006) Comment on "Changes in tropical cyclone number, duration, and intensity in a warming environment". *Science* 311(5768):1713–1713. <https://doi.org/10.1126/science.1121522>
- Chand SS, Walsh KJ, Camargo SJ, Kossin JP, Tory KJ, Wehner MF, Chan CLJ, Klotzbach JP, Dowdy AJ, Bell SS, Ramsay HA, Murakami H (2022) Declining tropical cyclone frequency under global warming. *Nat Clim Change* 12(7):655–661. <https://doi.org/10.1038/s41558-022-01388-4>

- Chang EKM, Guo Y (2007) Is the number of North Atlantic tropical cyclones significantly underestimated prior to the availability of satellite observations? *Geophys Res Lett* 34:L14801. <https://doi.org/10.1029/2007GL030169>
- Chan JC (2009) Thermodynamic control on the climate of intense tropical cyclones. *Proc Math Phys Eng Sci* 465(2110):3011–3021. <https://doi.org/10.1098/rspa.2009.0114>
- Choi W, Ho CH, Kim J, Kim HS, Feng S, Kang K (2016) A track pattern-based seasonal prediction of tropical cyclone activity over the North Atlantic. *J Clim* 29(2):481–494. <https://doi.org/10.1175/JCLI-D-15-0407.1>
- Chu J-H, Sampson CR, Levine AS, and Fukada E (2002) The Joint typhoon warning center best-tracks, 1945–2000. Naval Research Laboratory Reference Number NRL/MR/7540–02–16. Retrieved from <https://www.metoc.navy.mil/jtwc/products/best-tracks/tc-bt-report.html>. Accessed on 23 Jan 2023
- Chu P-S, Murakami H (2022) *Climate Variability and Tropical Cyclone Activity*. Cambridge University Press, Cambridge, UK, p 320
- Dai A, Rasmussen RM, Ikeda K, Liu C (2020) A new approach to construct representative future forcing data for dynamic downscaling. *Clim Dyn* 55(1):315–323. <https://doi.org/10.1007/s00382-017-3708-8>
- Delfino RJ, Vidale PL, Bagtasa G, Hodges K (2023) Response of damaging Philippines tropical cyclones to a warming climate using the pseudo global warming approach. *Clim Dyn* 1–25 <https://doi.org/10.1007/s00382-023-06742-6>
- Dwyer JG, Camargo SJ, Sobel AH, Biasutti M, Emanuel KA, Vecchi GA, Zhao M, Tippett MK (2015) Projected twenty-first-century changes in the length of the tropical cyclone season. *J Clim* 28(15):6181–6192. <https://doi.org/10.1175/JCLI-D-14-00686.1>
- Elsner JB, Kossin JP, Jagger TH (2008) The increasing intensity of the strongest tropical cyclones. *Nature* 455(7209):92–95. <https://doi.org/10.1038/nature07234>
- Emanuel KA (2004) Tropical cyclone energetics and structure. In: Fedorovich E, Rotunno R, Stevens B (eds) *Atmospheric Turbulence and Mesoscale Meteorology*. Cambridge University Press, Cambridge, UK, pp 165–192
- Emanuel K, Sundararajan R, Williams J (2008) Hurricanes and global warming: Results from downscaling IPCC AR4 simulations. *Bull Am Meteorol Soc* 89(3):347–368. <https://doi.org/10.1175/BAMS-89-3-347>
- Emanuel K (2021a) Atlantic tropical cyclones downscaled from climate reanalyses show increasing activity over past 150 years. *Nat Commun* 12(1):1–8. <https://doi.org/10.1038/s41467-021-27364-8>
- Emanuel K (2021b) Response of global tropical cyclone activity to increasing CO₂: results from downscaling CMIP6 models. *J Clim* 34(1):57–70. <https://doi.org/10.1175/JCLI-D-20-0367.1>
- Emanuel K, Sobel A (2013) Response of tropical sea surface temperature, precipitation, and tropical cyclone-related variables to changes in global and local forcing. *J Adv Model Earth Syst* 5:447–458. <https://doi.org/10.1002/jame.20032>
- Emanuel KA (1986) An air-sea interaction theory for tropical cyclones. Part I: Steady-state maintenance. *J Atmos Sci* 43(6):585–605 [https://doi.org/10.1175/1520-0469\(1986\)043<0585:AASTIF>2.0.CO;2](https://doi.org/10.1175/1520-0469(1986)043<0585:AASTIF>2.0.CO;2)
- Emanuel KA (2000) A statistical analysis of hurricane intensity. *Mon Wea Rev* 128:1139–1152. [https://doi.org/10.1175/1520-0493\(2000\)128%3c1139:ASAOTC%3e2.0.CO;2](https://doi.org/10.1175/1520-0493(2000)128%3c1139:ASAOTC%3e2.0.CO;2)
- Eyring V, Bony S, Meehl GA, Senior CA, Stevens B, Stouffer RJ, Taylor KE (2016) Overview of the Coupled Model Intercomparison Project Phase 6 (CMIP6) experimental design and organization. *Geosci Model Dev* 9:1937–1958. <https://doi.org/10.5194/gmd-9-1937-2016>
- Fernández-Alvarez JC, Díaz-Rodríguez O, Pérez-Alarcón A (2019) Proposal of Pressure Calculation Method for a Model of Potential Intensity. *Rev Bras Meteorol* 34:101–108. <https://doi.org/10.1590/0102-7786334013>
- Frank W, Ritchie E (2001) Effects of vertical wind shear on the intensity and structure of numerically simulated hurricanes. *Mon Wea Rev* 129:2249–2269. [https://doi.org/10.1175/1520-0493\(2001\)129%3c2249:EOVWSO%3e2.0.CO;2](https://doi.org/10.1175/1520-0493(2001)129%3c2249:EOVWSO%3e2.0.CO;2)
- Fraza E, Elsner JB (2015) A climatological study of the effect of sea-surface temperature on North Atlantic hurricane intensification. *Phys Geogr* 36(5):395–407. <https://doi.org/10.1080/02723646.2015.1066146>
- Fu Y, Lin Z, Wang T (2021) Simulated Relationship between Wintertime ENSO and East Asian Summer Rainfall: From CMIP3 to CMIP6. *Adv Atmos Sci* 38:221–236. <https://doi.org/10.1007/s00376-020-0147-y>
- Gallina V, Torresan S, Critto A, Sperotto A, Glade T, Marcomini A (2016) A review of multi-risk methodologies for natural hazards: Consequences and challenges for a climate change impact assessment. *J Environ Manage* 168:123–132. <https://doi.org/10.1016/j.jenvman.2015.11.011>
- Ge X, Li T, Peng M (2013) Effects of vertical shears and midlevel dry air on tropical cyclone developments. *J Atmos Sci* 70:3859–3875. <https://doi.org/10.1175/JAS-D-13-066.1>

- Gilford DM, Solomon S, Emanuel KA (2017) On the seasonal cycles of tropical cyclone potential intensity. *J Clim* 30(16):6085–6096. <https://doi.org/10.1175/JCLI-D-16-0827.1>
- Gilford DM, Solomon S, Emanuel KA (2019) Seasonal cycles of along-track tropical cyclone maximum intensity. *Mon Wea Rev* 147(7):2417–2432. <https://doi.org/10.1175/MWR-D-19-0021.1>
- Grise KM, Davis SM, Staten PW, Adam O (2018) Regional and seasonal characteristics of the recent expansion of the tropics. *J Clim* 31(17):6839–6856. <https://doi.org/10.1175/JCLI-D-18-0060.1>
- Guo YP, Tan ZM (2018) Westward migration of tropical cyclone rapid-intensification over the North-western Pacific during short duration El Niño. *Nat Commun* 9(1):1–10. <https://doi.org/10.1038/s41467-018-03945-y>
- Held IM, Guo H, Adcroft A, Dunne JP, Horowitz LW, Krasting J, et al. (2019) Structure and performance of GFDL's CM4. 0 climate model. *J Adv Model Earth Syst* 11(11):3691–3727 <https://doi.org/10.1029/2019MS001829>
- Held IM, Soden BJ (2006) Robust responses of the hydrological cycle to global warming. *J Clim* 19(21):5686–5699. <https://doi.org/10.1175/JCLI3990.1>
- Hersbach H, Bell B, Berrisford P, Hirahara S, Horányi A, Muñoz-Sabater J et al (2020) The ERA5 global reanalysis. *Q J R Meteorol* 146(730):1999–2049. <https://doi.org/10.1002/qj.3803>
- Holland G, Bruyère CL (2014) Recent intense hurricane response to global climate change. *Clim Dyn* 42(3):617–627. <https://doi.org/10.1007/s00382-013-1713-0>
- Hoque MAA, Phinn S, Roelfsema C, Childs I (2017a) Modelling tropical cyclone risks for present and future climate change scenarios using geospatial techniques. *Int J Digit Earth* 11(3):246–263. <https://doi.org/10.1080/17538947.2017.1320595>
- Hoque MAA, Phinn S, Roelfsema C (2017b) A systematic review of tropical cyclone disaster management research using remote sensing and spatial analysis. *Ocean Coast Manag* 146:109–120. <https://doi.org/10.1016/j.ocecoaman.2017.07.001>
- Hoque MAA, Phinn S, Roelfsema C, Childs I (2017c) Tropical cyclone disaster management using remote sensing and spatial analysis: A review. *Int J Disaster Risk Reduct* 22:345–354. <https://doi.org/10.1016/j.ijdr.2017.02.008>
- Jones SC (1995) The evolution of vortices in vertical shear. I: Initially barotropic vortices. *QJR Meteorol* 121(524):821–851 <https://doi.org/10.1002/qj.49712152406>
- Kieu C, Zhang DL (2018) The control of environmental stratification on the hurricane maximum potential intensity. *Geophys Res Lett* 45(12):6272–6280. <https://doi.org/10.1029/2018GL078070>
- Kieu CQ, Wang Q (2017a) Stability of hurricane maximum potential intensity. *J Atmos Sci* 74(11):3591–3608. <https://doi.org/10.1175/JAS-D-17-0028.1>
- Kieu CQ, Wang Q (2017b) On the scale dynamics of tropical cyclone intensity. *Discrete Continuous Dyn Syst Ser B* 22(5):44–54. <https://doi.org/10.3934/dcdsb.2017196>
- Killick R, Fearhead P, Eckley IA (2012) Optimal detection of changepoints with a linear computational cost. *Am Stat Assoc* 107(500):1590–1598. <https://doi.org/10.1080/01621459.2012.737745>
- Kim HS, Ho CH, Kim JH, Chu PS (2012) Track-pattern-based model for seasonal prediction of tropical cyclone activity in the western North Pacific. *J Clim* 25(13):4660–4678. <https://doi.org/10.1175/JCLI-D-11-00236.1>
- Klotzbach PJ, Bowen SG, Pielke R, Bell M (2018) Continental US hurricane landfall frequency and associated damage: Observations and future risks. *Bull Am Meteorol Soc* 99(7):1359–1376. <https://doi.org/10.1175/bams-d-17-0184.1>
- Klotzbach PJ, Landsea CW (2015) Extremely intense hurricanes: revisiting Webster et al. (2005) after 10 years. *J Clim* 28(19):7621–7629. <https://doi.org/10.1175/JCLI-D-15-0188.1>
- Klotzbach PJ, Wood KM, Schreck III CJ, Bowen SG, Patricola CM, Bell MM (2022) Trends in Global Tropical Cyclone Activity: 1990–2021. *Geophys Res Lett* 49(6):e2021GL095774 <https://doi.org/10.1029/2021GL095774>
- Knapp KR, Kruk MC, Levinson DH, Diamond HJ, Neumann CJ (2010) The international best track archive for climate stewardship (IBTrACS) unifying tropical cyclone data. *Bull Am Meteorol Soc* 91(3):363–376. <https://doi.org/10.1175/2009BAMS2755.1>
- Knapp KR, Diamond HJ, Kossin JP, Kruk MC, and Schreck CJ (2018) International best track archive for climate stewardship (IBTrACS) Project, Version 4. NOAA National Centers for Environmental Information. <https://doi.org/10.25921/82ty-9e16>. Accessed 29 Jan 2023
- Knutson T, Camargo SJ, Chan JC, Emanuel K, Ho CH, Kossin J et al (2019) Tropical cyclones and climate change assessment: Part I: Detection and attribution. *Bull Am Meteorol Soc* 100(10):1987–2007. <https://doi.org/10.1175/BAMS-D-18-0189.1>
- Knutson T, Camargo SJ, Chan JCL, Emanuel K, Ho C, Kossin J, Mohapatra M, Satoh M, Sugi M, Walsh K, and Wu L (2020) Tropical Cyclones and Climate Change Assessment: Part II: Projected Response

- to Anthropogenic Warming. *Bull Am Meteorol Soc* 101(3):E303–E322 <https://doi.org/10.1175/BAMS-D-18-0194.1>
- Knutson TR, Sirutis JJ, Vecchi GA, Garner S, Zhao M, Kim HS et al (2013) Dynamical downscaling projections of twenty-first-century Atlantic hurricane activity: CMIP3 and CMIP5 model-based scenarios. *J Clim* 26(17):6591–6617. <https://doi.org/10.1175/JCLI-D-12-00539.1>
- Korty RL, Emanuel KA, Scott JR (2008) Tropical cyclone-induced upper-ocean mixing and climate: application to equable climates. *J Clim* 21:638–654. <https://doi.org/10.1175/2007JCLI1659.1>
- Kossin JP, Olander TL, Knapp KR (2013) Trend analysis with a new global record of tropical cyclone intensity. *J Clim* 26(24):9960–9976. <https://doi.org/10.1175/JCLI-D-13-00262.1>
- Kossin JP, Knapp KR, Olander TL, Velden CS (2020) Global increase in major tropical cyclone exceedance probability over the past four decades. *Proc Natl Acad Sci* 117(22):11975–11980. <https://doi.org/10.1073/pnas.1920849117>
- Kossin JP (2017) Hurricane intensification along United States coast suppressed during active hurricane periods. *Nature* 541(7637):390–393. <https://doi.org/10.1038/nature20783>
- Kossin JP, Camargo SJ (2009) Hurricane track variability and secular potential intensity trends. *Clim Change* 97:329–337. <https://doi.org/10.1007/s10584-009-9748-2>
- Kowaleski AM, Evans JL (2016) A reformulation of tropical cyclone potential intensity theory incorporating energy production along a radial trajectory. *Mon Wea Rev* 144(10):3569–3578. <https://doi.org/10.1175/MWR-D-15-0383.1>
- Lai Y, Dzombak DA (2019) Use of historical data to assess regional climate change. *J Clim* 32(14):4299–4320. <https://doi.org/10.1175/JCLI-D-18-0630.1>
- Landsea CW, Franklin JL (2013) Atlantic hurricane database uncertainty and presentation of a new database format. *Mon Wea Rev* 141(10):3576–3592. <https://doi.org/10.1175/mwr-d-12-00254.1>
- Lee CY, Camargo SJ, Sobel AH, Tippett MK (2020) Statistical–dynamical downscaling projections of tropical cyclone activity in a warming climate: Two diverging genesis scenarios. *J Clim* 33(11):4815–4834. <https://doi.org/10.1175/JCLI-D-19-0452.1>
- Li C, Lu R, Chen G (2017) Promising prediction of the monsoon trough and its implication for tropical cyclone activity over the western North Pacific. *Environ Res Lett* 12(7):074027 <https://doi.org/10.1088/1748-9326/aa71bd>
- Li W, Li L, Deng Y (2015) Impact of the interdecadal Pacific oscillation on tropical cyclone activity in the North Atlantic and eastern North Pacific. *Sci Rep* 5(1):12358. <https://doi.org/10.1038/srep12358>
- Li JL, Xu KM, Jiang JH, Lee WL, Wang LC, Yu JY, et al. (2020) An overview of CMIP5 and CMIP6 simulated cloud ice, radiation fields, surface wind stress, sea surface temperatures, and precipitation over tropical and subtropical oceans. *J Geophys Res Atmos* 125(15):e2020JD032848 <https://doi.org/10.1029/2020JD032848>
- Lockwood JW, Oppenheimer M, Lin N, Kopp RE, Vecchi GA, Gori A, (2022) Correlation Between Sea-Level Rise and Aspects of Future Tropical Cyclone Activity in CMIP6 Models. *Earth's Future* 10(4):e2021EF002462 <https://doi.org/10.1029/2021EF002462>
- Luo H, Han Y (2021) Impacts of the Saharan air layer on the physical properties of the Atlantic tropical cyclone cloud systems: 2003–2019. *Atmos Chem Phys* 21(19):15171–15184. <https://doi.org/10.5194/acp-21-15171-2021>
- Makarieva AM, Nefiodov AV (2023) A critical analysis of the assumptions underlying the formulation of maximum potential intensity for tropical cyclones. *J Atmos Sci* 80(4):1201–1209. <https://doi.org/10.1175/JAS-D-22-0144.1>
- Mendelsohn R, Emanuel K, Chonabayashi S, Bakkensen L (2012) The impact of climate change on global tropical cyclone damage. *Nat Clim Change* 2(3):205–209. <https://doi.org/10.1038/nclimate1357>
- Miyamoto Y, Bryan GH, Rotunno R (2017) An analytical model of maximum potential intensity for tropical cyclones incorporating the effect of ocean mixing. *Geophys Res Lett* 44(11):5826–5835. <https://doi.org/10.1002/2017GL073670>
- Moon IJ, Kim SH, Chan JC (2019) Climate change and tropical cyclone trend. *Nature* 570(7759):E3–E5. <https://doi.org/10.1038/s41586-019-1222-3>
- Murakami H, Delworth TL, Cooke WF, Zhao M, Xiang B, Hsu PC (2020) Detected climatic change in global distribution of tropical cyclones. *Proc Natl Acad Sci USA* 117(20):10706–10714. <https://doi.org/10.1073/pnas.1922500117>
- Murakami H, Hsu PC, Arakawa O, Li T (2014) Influence of model biases on projected future changes in tropical cyclone frequency of occurrence. *J Clim* 27(5):2159–2181. <https://doi.org/10.1175/JCLI-D-13-00436.1>
- Murakami H, Mizuta R, Shindo E (2012) Future changes in tropical cyclone activity projected by multi-physics and multi-SST ensemble experiments using the 60-km-mesh MRI-AGCM. *Clim Dyn* 39(9):2569–2584. <https://doi.org/10.1175/JCLI-D-11-00415.1>

- Nijssse FJ, Cox PM, Williamson MS (2020) (2020) An emergent constraint on Transient Climate Response from simulated historical warming in CMIP6 models. *Earth Syst Dynam* 11:737–750. <https://doi.org/10.5194/esd-11-737-2020>
- O'Neill BC, Krieglger E, Ebi K, Kemp-Benedict E, Riahi K, Rothman DS et al (2017) The roads ahead: narratives for shared socioeconomic pathways describing world futures in the 21st century. *Glob Environ Change* 42:169–180. <https://doi.org/10.1016/j.gloenvcha.2015.01.004>
- O'Gorman PA, and Muller CJ (2010) How closely do changes in surface and column water vapor follow Clausius–Clapeyron scaling in climate change simulations?. *Environ Res Lett* 5(2):025207 <https://doi.org/10.1088/1748-9326/5/2/025207>
- Park DSR, Kim HS, Kwon M, Byun YH, Kim MK, Chung IU et al (2021) A Performance Evaluation of Potential Intensity over the Tropical Cyclone Passage to South Korea Simulated by CMIP5 and CMIP6 Models. *Atmosphere* 12(9):1214. <https://doi.org/10.3390/atmos12091214>
- Pasquero C, Desbiolles F, Meroni AN (2021) Air-sea interactions in the cold wakes of tropical cyclones. *Geophys Res Lett* 48(2):e2020GL091185 <https://doi.org/10.1029/2020GL091185>
- Peduzzi P, Chatenoux B, Dao H, De Bono A, Herold C, Kossin J, Mouton F, Nordbeck O (2012) Global trends in tropical cyclone risk. *Nat Clim Change* 2:289–294. <https://doi.org/10.1038/nclimate1410>
- Pérez-Alarcón A, Fernández-Alvarez JC, Sorí R, Nieto R, and Gimeno L (2021a) The relationship of the sea surface temperature and climate variability modes with the North Atlantic tropical cyclones activity. *Rev Cub Meteorol* 27(3):1–15. <http://rcm.insmet.cu/index.php/rcm/article/view/575/1145>. Accessed 12 Feb 2023
- Pérez-Alarcón A, Fernández-Alvarez JC, Díaz-Rodríguez O (2021b) Hurricane maximum potential intensity and Global Warming. *Rev Cub Fis* 38(2):77–84. <http://www.revistacubanadefisica.org/index.php/rcf/article/view/RCF2021v38p077>. Accessed 18 Feb 2023
- Pérez-Alarcón A, Fernández-Alvarez JC, Díaz-Rodríguez O (2021c) Hurricane maximum potential intensity model. *Rev Cub Fis* 38(2):85–93. <http://www.revistacubanadefisica.org/index.php/rcf/article/view/2021v38p085>. Accessed 18 Feb 2023
- Pérez-Alarcón A, Fernández-Alvarez JC, and Díaz-Rodríguez O (2022) HuMPI: Hurricane Maximum Potential Intensity model (V1.0). Zenodo, Geneva, Switzerland. <https://doi.org/10.5281/zenodo.6475215>
- Pérez-Alarcón A, Fernández-Alvarez JC (2022) Climatological Variations in the Intensity of Tropical Cyclones Formed over the North Atlantic Basin Using the Hurricane Maximum Potential Intensity (HuMPI) Model. *Environ Sci Proc* 19(1):34. <https://doi.org/10.3390/ecas2022-12828>
- Poulos HM (2010) Spatially explicit mapping of hurricane risk in New England, USA using ArcGIS. *Nat Hazards* 54(3):1015–1023. <https://doi.org/10.1007/s11069-010-9502-0>
- Pun I-F, Lin I-I, Lo M-H (2013) Recent increase in high tropical cyclone heat potential area in the Western North Pacific Ocean. *Geophys Res Lett* 40:4680–4684. <https://doi.org/10.1002/grl.50548>
- Riahi K, Van Vuuren DP, Krieglger E, Edmonds J, O'neill BC, Fujimori S et al. (2017) The shared socioeconomic pathways and their energy, land use, and greenhouse gas emissions implications: an overview. *Glob Environ Change* 42:153–168 <https://doi.org/10.1016/j.gloenvcha.2016.05.009>
- Roberts MJ, Vidale PL, Senior C, Hewitt HT, Bates C, Berthou S et al (2018) The benefits of global high resolution for climate simulation: process understanding and the enabling of stakeholder decisions at the regional scale. *Bull Am Meteorol Soc* 99(11):2341–2359. <https://doi.org/10.1175/BAMS-D-15-00320.1>
- Roberts MJ, Camp J, Seddon J, Vidale PL, Hodges K, Vannièrè B et al. (2020) Projected future changes in tropical cyclones using the CMIP6 HighResMIP multimodel ensemble. *Geophys Res Lett* 47(14):e2020GL088662 <https://doi.org/10.1029/2020GL088662>
- Satoh M, Yamada Y, Sugi M, Kodama C, Noda AT (2015) Constraint on future change in global frequency of tropical cyclones due to global warming. *J Meteorol Soc Jpn Ser II* 93(4):489–500. <https://doi.org/10.2151/jmsj.2015-025>
- Sharma N, Varma AK (2022) Impact of vertical wind shear in modulating tropical cyclones eye and rainfall structure. *Nat Hazards* 112(3):2083–2100. <https://doi.org/10.1007/s11069-022-05257-3>
- Sharmila S, Walsh KJE (2018) Recent poleward shift of tropical cyclone formation linked to Hadley cell expansion. *Nat Clim Change* 8(8):730–736. <https://doi.org/10.1038/s41558-018-0227-5>
- Shen Y, Sun Y, Zhong Z, Liu K, Shi J (2018) Sensitivity Experiments on the Poleward Shift of Tropical Cyclones over the Western North Pacific under Warming Ocean Conditions. *J Meteor Res* 32(4):560–570. <https://doi.org/10.1007/s13351-018-8047-0>
- Shi D, Ge X, Peng M (2019) Latitudinal dependence of the dry air effect on tropical cyclone development. *Dyn Atmos Oceans* 87:101102 <https://doi.org/10.1016/j.dynatmoce.2019.101102>
- Shu S, Wu L (2009) Analysis of the influence of Saharan air layer on tropical cyclone intensity using AIRS/Aqua data. *Geophys Res Lett* 36:L09809. <https://doi.org/10.1029/2009GL037634>
- Shultz JM, Russell J, Espinel Z (2005) Epidemiology of tropical cyclones: the dynamics of disaster, disease, and development. *Epidemiol Rev* 27(1):21–35. <https://doi.org/10.1093/epirev/mxi011>

- Smith RK (2003) A simple model of the hurricane boundary layer. *QJR Meteorol* 129(589):1007–1027. <https://doi.org/10.1256/qj.01.197>
- Smith RK, Vogl S (2008) A simple model of the hurricane boundary layer revisited. *QJR Meteorol* 134(631):337–351. <https://doi.org/10.1002/qj.216>
- Smith RK, Montgomery MT, Vogl S (2008) A critique of Emanuel's hurricane model and potential intensity theory. *QJR Meteorol Soc* 134(632):551–561. <https://doi.org/10.1002/qj.241>
- Sobel AH, Wing AA, Camargo SJ, Patricola CM, Vecchi GA, Lee CY, Tippett MK (2021) Tropical cyclone frequency. *Earth's Future* 9(12):e2021EF002275 <https://doi.org/10.1029/2021EF002275>
- Sobel AH, Camargo SJ, Hall TM, Lee CY, Tippett MK, Wing AA (2016) Human influence on tropical cyclone intensity. *Science* 353(6296):242–246. <https://doi.org/10.1126/science.aaf6574>
- Song J, Klotzbach PJ (2018) What has controlled the poleward migration of annual averaged location of tropical cyclone lifetime maximum intensity over the western North Pacific since 1961? *Geophys Res Lett* 45(2):1148–1156. <https://doi.org/10.1002/2017GL076883>
- Studholme J, Fedorov AV, Gulev SK, Emanuel K, Hodges K (2022) Poleward expansion of tropical cyclone latitudes in warming climates. *Nat Geosci* 15(1):14–28. <https://doi.org/10.1038/s41561-021-00859-1>
- Sun J, Wang D, Hu X, Ling Z, Wang L (2019) Ongoing poleward migration of tropical cyclone occurrence over the western North Pacific Ocean. *Geophys Res Lett* 46:9110–9117. <https://doi.org/10.1029/2019GL084260>
- Tang B, Emanuel K (2010) Midlevel ventilation's constraint on tropical cyclone intensity. *J Atmos Sci* 67(6):1817–1830. <https://doi.org/10.1175/2010JAS3318.1>
- Tao D, Zhang F (2014) Effect of environmental shear, sea-surface temperature, and ambient moisture on the formation and predictability of tropical cyclones: An ensemble-mean perspective. *J Adv Model Earth Syst* 6:384–404. <https://doi.org/10.1002/2014MS000314>
- Thompson C, Barthe C, Bielli S, Tulet P, Pianezze J (2021) Projected Characteristic Changes of a Typical Tropical Cyclone under Climate Change in the South West Indian Ocean. *Atmosphere* 12(2):232. <https://doi.org/10.3390/atmos12020232>
- Vecchi GA, Knutson TR (2008) On estimates of historical North Atlantic tropical cyclone activity. *J Clim* 21(14):3580–3600. <https://doi.org/10.1175/2008JCLI2178.1>
- Vecchi GA, Landsea C, Zhang W, Villarini G, Knutson T (2021) Changes in Atlantic major hurricane frequency since the late-19th century. *Nat Commun* 12(1):1–9. <https://doi.org/10.1038/s41467-021-24268-5>
- Vecchi GA, Delworth TL, Murakami H, Underwood SD, Wittenberg AT, Zeng F et al (2019) Tropical cyclone sensitivities to CO2 doubling: Roles of atmospheric resolution, synoptic variability and background climate changes. *Clim Dyn* 53:5999–6033. <https://doi.org/10.1007/s00382-019-04913-y>
- Walsh KJ, McBride JL, Klotzbach PJ, Balachandran S, Camargo SJ, Holland G et al (2016) Tropical cyclones and climate change. *Wiley Interdiscip Rev Clim Change* 7(1):65–89. <https://doi.org/10.1002/wcc.371>
- Walsh KJ, Camargo SJ, Knutson TR, Kossin J, Lee TC, Murakami H, Patricola C (2019) Tropical cyclones and climate change. *Trop Cyclone Res Rev* 8(4):240–250. <https://doi.org/10.1016/j.tcrr.2020.01.004>
- Wang YF, Tan ZM (2022) Essential dynamics of the vertical wind shear affecting the secondary eyewall formation in tropical cyclones. *J Atmos Sci* 79(11):2831–2847. <https://doi.org/10.1175/JAS-D-21-0340.1>
- Wang S, Toumi R (2019) Impact of dry midlevel air on the tropical cyclone outer circulation. *J Atmos Sci* 76(6):1809–1826. <https://doi.org/10.1175/JAS-D-18-0302.1>
- Wang S, Camargo SJ, Sobel AH, Polvani LM (2014) Impact of the tropopause temperature on the intensity of tropical cyclones: An idealized study using a mesoscale model. *J Atmos Sci* 71:4333–4348. <https://doi.org/10.1175/JAS-D-14-0029.1>
- Webster PJ, Holland GJ, Curry JA, Chang HR (2005) Changes in tropical cyclone number, duration, and intensity in a warming environment. *Science* 309(5742):1844–1846. <https://doi.org/10.1126/science.1116448>
- Wehner M, Reed KA, Stone D, Collins WD, Bacmeister J (2015) Resolution dependence of future tropical cyclone projections of CAM5. 1 in the US CLIVAR Hurricane Working Group idealized configurations. *J Clim* 28(10):3905–3925 <https://doi.org/10.1175/JCLI-D-14-00311.1>
- Willoughby HE, Darling RWR, and Rahn ME (2006) Parametric representation of the primary hurricane vortex. Part II: A new family of sectionally continuous profiles. *Mon Weather Rev* 134(4):1102–1120 <https://doi.org/10.1175/MWR3106.1>
- Wing AA, Emanuel K, Solomon S (2015) On the factors affecting trends and variability in tropical cyclone potential intensity. *Geophys Res Lett* 42(20):8669–8677. <https://doi.org/10.1002/2015GL066145>
- Wing AA, Sobel AH, Camargo SJ (2007) Relationship between the potential and actual intensities of tropical cyclones on interannual time scales. *Geophys Res Lett* 34:L08810. <https://doi.org/10.1029/2006GL028581>

- Widhalm M, Hamlet A, Byun K, Robeson S, Baldwin M, Staten P, Chiu C, et al. (2018) Indiana's Past & Future Climate: A Report from the Indiana Climate Change Impacts Assessment. Purdue Climate Change Research Center, Purdue University, West Lafayette, Indiana. <https://doi.org/10.5703/1288284316634>
- Wu L, Zhao H, Wang C, Cao J, Liang J (2022) Understanding of the effect of climate change on tropical cyclone intensity: a review. *Adv Atmos Sci* 39(2):205–221. <https://doi.org/10.1007/s00376-021-1026-x>
- Wu CC, Emanuel KA (1993) Interaction of a baroclinic vortex with background shear: Application to hurricane movement. *J Atmos Sci* 50(1):62–76. [https://doi.org/10.1175/1520-0469\(1993\)050%3c0062:IOABVW%3e2.0.CO;2](https://doi.org/10.1175/1520-0469(1993)050%3c0062:IOABVW%3e2.0.CO;2)
- Wu L, Chou C, Chen CT, Huang R, Knutson TR, Sirutis JJ et al (2014) Simulations of the present and late-twenty-first-century western North Pacific tropical cyclone activity using a regional model. *J Clim* 27(9):3405–3424. <https://doi.org/10.1175/JCLI-D-12-00830.1>
- Xu Z, Han Y, Tam C, Yang ZL, Fu C (2021) Bias-corrected CMIP6 global dataset for dynamical downscaling of the historical and future climate (1979–2100). *Sci Data* 8(1):1–11. <https://doi.org/10.1038/s41597-021-01079-3>
- Yang L, Cheng X, Huang X, Fei J, Li X, (2020) Effects of air-sea interaction on the eyewall replacement cycle of Typhoon Sinlaku (2008): Verification of numerical simulation. *Earth Space Sci* 7(2):e2019EA000763 <https://doi.org/10.1029/2019EA000763>
- Yang X, Huang P (2022) Improvements in the relationship between tropical precipitation and sea surface temperature from CMIP5 to CMIP6. *Clim Dyn*. <https://doi.org/10.1007/s00382-022-06519-3>
- Yan X, Zhang R, Knutson TR (2017) The role of Atlantic overturning circulation in the recent decline of Atlantic major hurricane frequency. *Nat Commun* 8(1):1695. <https://doi.org/10.1038/s41467-017-01377-8>
- Yin J, Yin Z, Xu S (2013) Composite risk assessment of typhoon-induced disaster for China's coastal area. *Nat Hazards* 69(3):1423–1434. <https://doi.org/10.1007/s11069-013-0755-2>
- Zelinka MD, Myers TA, McCoy DT, Po-Chedley S, Caldwell PM, Ceppi P, Klein SA, Taylor KE (2020) Causes of higher climate sensitivity in CMIP6 models. *Geophys Res Lett* 47:e2019GL085782 <https://doi.org/10.1029/2019GL085782>
- Zhang W-Q, Wu L-G, Zou X-K (2018) Changes of tropical cyclone tracks in the western North Pacific over 1979–2016. *Adv Clim Change Res* 9(3):170–176. <https://doi.org/10.1016/j.accre.2018.06.002>
- Zhao M, Held IM (2012) TC-permitting GCM simulations of hurricane frequency response to sea surface temperature anomalies projected for the late-twenty-first century. *J Clim* 25(8):2995–3009. <https://doi.org/10.1175/JCLI-D-11-00313.1>
- Zhou S, Huang G, Huang P (2020) Excessive ITCZ but negative SST biases in the tropical Pacific simulated by CMIP5/6 models: The role of the meridional pattern of SST bias. *J Clim* 33(12):5305–5316. <https://doi.org/10.1175/JCLI-D-19-0922.1>

Publisher's Note Springer Nature remains neutral with regard to jurisdictional claims in published maps and institutional affiliations.

Authors and Affiliations

Albenis Pérez-Alarcón^{1,2}  · José C. Fernández-Alvarez^{1,2}  · Patricia Coll-Hidalgo^{1,3} 

✉ Albenis Pérez-Alarcón
albenis.perez.alarcon@uvigo.es

¹ Centro de Investigación Mariña, Universidade de Vigo, Environmental Physics Laboratory (EPhysLab), Campus As Lagoas s/n, Ourense 32004, Spain

² Departamento de Meteorología, Instituto Superior de Tecnologías Y Ciencias Aplicadas, Universidad de La Habana, La Habana 10400, Cuba

³ Oficina Principal de Vigilancia Meteorológica, Empresa Cubana de Navegación Aérea, Carretera Panamericana Y Final, La Habana, Boyeros 10800, Cuba